

Optical transitions in Ge/SiGe multiple quantum wells with Ge-rich barriers

M. Bonfanti, E. Grilli, and M. Guzzi

*CNISM and L-NESS, Dipartimento di Scienza dei Materiali, Università degli Studi di Milano-Bicocca,
Via Cozzi 53, I-20125 Milano, Italy*

M. Virgilio and G. Grosso

*NEST-INFN, Piazza San Silvestro 12, 5612 Pisa, Italy and Dipartimento di Fisica "E. Fermi,"
Università di Pisa, Largo Pontecorvo 3, I-56127 Pisa, Italy*

D. Chrastina, G. Isella, and H. von Känel

*CNISM and L-NESS, Dipartimento di Fisica del Politecnico di Milano, Polo di Como,
Via Anzani 42, I-22100 Como, Italy*

A. Neels

Institute of Microtechnology, University of Neuchâtel, Rue Jaquet-Droz 1, CH-2002 Neuchâtel, Switzerland

(Received 25 June 2008; published 25 July 2008)

Direct-gap and indirect-gap transitions in strain-compensated Ge/SiGe multiple quantum wells with Ge-rich SiGe barriers have been studied by optical transmission spectroscopy and photoluminescence experiments. An $sp^3d^5s^*$ tight-binding model has been adopted to interpret the experimental results. Photoluminescence spectra and their comparison with theoretical calculations prove the existence of type-I band alignment in compressively strained Ge quantum wells grown on relaxed Ge-rich SiGe buffers. The high quality of the transmission spectra opens up other perspectives for application of these structures in near-infrared optical modulators.

DOI: [10.1103/PhysRevB.78.041407](https://doi.org/10.1103/PhysRevB.78.041407)

PACS number(s): 78.67.De, 73.21.Fg

Knowledge of the band lineup at semiconductor hetero-interfaces is one of the key requirements for understanding the physical properties of quantum-confined structures and their device applications. The band lineups in heterostructures containing SiGe layers are of particular relevance in view of the compatibility of this material system with Si processing.

In low Ge content SiGe-based quantum wells (QWs) strained to the Si lattice parameter, a long debate originally favoring type I (Refs. 1–3) was finally settled in terms of type-II band alignment.⁴ Indeed, most of the papers devoted to the optical and electronic properties of SiGe-based heterostructures addressed alloys pseudomorphically grown on Si with a Ge mole fraction of typically $x_{\text{Ge}} < 0.30$ – 0.50 .^{1–7} This was due to the difficult growth of strained Ge-rich heterostructures, requiring relaxed alloy buffer layers with a high Ge content in order to avoid strain release.⁸ No *experimental* information is therefore available in the literature concerning band alignment at Ge-rich heterointerfaces. Recently, however, Ge-rich heterostructures of exceptional quality have become available for experimental studies of optical and electronic properties, thanks to innovative epitaxial growth techniques, such as low-energy plasma-enhanced chemical vapor deposition (LEPECVD).⁹ SiGe heterostructures of high Ge content are of particular interest because their optical properties are expected to exhibit close analogies to those of direct-gap semiconductors, thanks to the proximity of the direct Γ and indirect L gaps.¹⁰ Indeed, strong quantum-confined Stark effect associated with interband transitions between zone-center states has been demonstrated in Ge/SiGe multiple quantum wells (MQWs).^{11,12} On the other hand, information on the lineup of the lowest conduction band with L character is purely theoretical.^{8,13,14} In view of the importance of the band lineup in MQW structures for

Si-based photonics,^{11,12,15} spintronics,¹⁶ and quantum computing,¹⁷ an experimental confirmation of these theoretical predictions appears highly desirable.

Proving the type-I band alignment in Ge-rich heterostructures strained to SiGe buffer layers of high Ge content is the main scope of this Rapid Communication. To this end, high-resolution absorption and photoluminescence (PL) spectra were combined with tight-binding calculations known to be very efficient in treating band alignment¹⁴ as well as inter- and intra-sub-band transitions in SiGe multilayer structures.¹⁸

The samples were grown by LEPECVD on 100 mm Si(100) substrates with a resistivity of 1–10 Ω cm. The first part of the structure was a buffer layer graded from Si to $\text{Si}_{0.1}\text{Ge}_{0.9}$ over a thickness of 13 μm and capped with a 2 μm $\text{Si}_{0.1}\text{Ge}_{0.9}$ layer. This formed a fully relaxed virtual substrate (VS). The MQW structure of samples 7864 and 7909 consisted of 200 Ge QWs with SiGe barriers whose nominal Ge mole fraction was $x_{\text{Ge}}=0.85$. For sample 7873 the number of periods was increased to 1000. Individual layer thicknesses were designed in order to balance the compressive strain in the QWs with the tensile strain in the barriers. The actual well and barrier thicknesses and the barrier composition were determined by high-resolution x-ray diffraction because in practice the growth rate is highly nonuniform across the wafer. As a result of this nonuniformity, many samples were actually available from each wafer with different well and barrier thicknesses but equal alloy compositions. Since MQW structures containing 200 and 1000 wells are more than 6 and 30 μm thick, respectively, for wafers 7873 and 7909 we attempted to limit the growth time by using high deposition rates (4–6 nm/s) for buffer⁹ and active layers. Thus LEPECVD growth of the whole structure of wafer 7909, including graded buffer and 200 QWs, was

TABLE I. Characteristics of the samples used in this work as obtained from the x-ray analysis. The thickness and the Ge content of QWs and barriers and the Ge content of graded VSs are reported. ε_{\parallel} and ε_{\perp} give the QW strain in the growth plane and perpendicular to it, respectively.

Sample	Growth rate		QW		Barrier		VS	ε_{\parallel}	ε_{\perp}
	(nm s ⁻¹)	No. of periods	d (nm)	x_{Ge}	d (nm)	x_{Ge}	x_{Ge}	(10 ⁻³)	(10 ⁻³)
7873-5	4–6	1000	5.4 ± 1.0	1.00	6.6	0.87	0.89	−4.8	3.6
7873-3	4–6	1000	19.9 ± 1.0	1.00	24.1	0.87	0.89	−4.8	3.6
7909-11	4–6	200	22.6 ± 1.0	1.00	27.3	0.87	0.89	−4.8	3.6
7864-1	0.3	200	3.8 ± 0.5	1.00	7.7	0.83	0.90	−4.5	3.4
7864-3	0.3	200	6.1 ± 1.0	1.00	12.3	0.83	0.90	−4.5	3.4
7864-5	0.3	200	8.5 ± 1.0	1.00	17.0	0.83	0.90	−4.5	3.4
7864-10	0.3	200	9.9 ± 1.0	1.00	22.8	0.82	0.89	−5.0	3.7

completed in a single run of just over 1 h. By contrast, the MQWs of wafer 7864 were grown at a rate of 0.3 nm/s. VSs with the same design but without MQW layers were used as reference samples for the transmission measurements.

The x-ray diffraction measurements were carried out with a PANalytical X'Pert PRO diffractometer using a Goebel mirror and a Bartels four-crystal monochromator on the primary beam path and a triple crystal analyzer in front of a proportional x-ray detector. High-resolution ω - 2θ scans and reciprocal space mapping were performed in the vicinity of the (004) and (115) reflections. The structural characteristics of the samples studied in this work are reported in Table I. The optical transmission measurements were performed at $T=300$ K and at $T=2$ K using a Jasco FT/IR-800 Fourier transform spectrometer equipped with an InGaAs detector. The measured optical density (OD) is defined as $\text{OD}(\lambda) = -\log_{10}[I_{\text{TS}}(\lambda)/I_{\text{TR}}(\lambda)]$, where $I_{\text{TS}}(\lambda)$ is the transmission spectrum of the sample and $I_{\text{TR}}(\lambda)$ is that of the reference sample, both measured on samples with mirror polished back surface. The absorption coefficient was deduced from the OD by using the total thickness of the Ge MQWs. For PL measurements the same Fourier transform spectrometer equipped with an InGaAs detector and a Peltier cooled PbS detector was used. Samples were excited using the 1064 nm line of a Nd-doped yttrium aluminum garnet (YAG) laser with an exciting power density of about 3 kW cm⁻². At this high excitation intensity, temperature control during PL measurements was achieved by immersion of the samples in superfluid liquid He.

To interpret the experimental results, electronic states and interband absorption were evaluated by means of a first-neighbor tight-binding Hamiltonian with $sp^3d^5s^*$ orbitals and spin-orbit interaction. The fundamental cell contains a number of atomic layers corresponding to one barrier and one well region and periodic boundary conditions are applied both along and orthogonal to the growth direction. Self-energies and hopping energies were chosen to reproduce the band structure of relaxed Si and Ge bulk crystals.¹⁹ Strain effects were then taken into account by means of elasticity theory and scaling the tight-binding hopping parameters according to the modified interatomic distances. Alloying in the barrier region was described by the virtual-crystal approximation. Band alignment along the growth direction was con-

sidered in the model adding a constant term to the site energies in the barrier region. The value of this term was chosen so as to reproduce the proper discontinuity in the valence band (VB) as explained in Ref. 14. Interband absorption due to vertical transitions was evaluated by sampling the two-dimensional (2D) Brillouin zone in a neighborhood of the Γ point as described in Ref. 18, where technical details of the method are discussed.

The optical spectra turned out to be of comparable quality for all samples cut from wafers 7864, 7873, and 7909. Then, in the following we shall focus on the 7864-10 sample, with 9.9-nm-thick wells and 22.8-nm-thick barriers.

The transmission spectra measured at room temperature and at $T=2$ K and the theoretical low-temperature spectrum calculated including excitonic effects are shown in Fig. 1. They are characterized by high value OD features, typical of confined excitons, much better defined than those reported for analogous structures.^{11,12} To interpret the near-gap absorption, we show in the inset of Fig. 1 the band-edge profiles at the Γ and L points and the confined states obtained from the diagonalization of the multilayer Hamiltonian. The arrows in Fig. 1 indicate the calculated transition energies between QW states at Γ , without excitonic effects. The peaks in the transmission spectra can thus be attributed to dipole-allowed $\text{HH}n\text{-c}\Gamma n$, $\text{LH}n\text{-c}\Gamma n$, and $\text{SO}n\text{-c}\Gamma n$ transitions. Here, $\text{HH}n$, $\text{LH}n$, and $\text{SO}n$ indicate heavy- and light-hole and split-off valence states at Γ , respectively, and $\text{c}\Gamma n$ indicate conduction states at Γ . All of them are confined in the Ge region with a type-I band-edge profile. In the transmission spectra, no clear evidence was found of the expected indirect transitions at lower energies between confined hole states at Γ and conduction-band (CB) states at the L point.

The half-width at half maximum (HWHM) of the $\text{HH1-c}\Gamma 1$ excitonic absorption line at $T=2$ K is about 4 meV, which compares well with the width of excitonic absorption lines reported in one of the first papers published on GaAs/AlGaAs MQWs of similar thickness.²⁰ The HWHM of the $\text{HH1-c}\Gamma 1$ excitonic absorption at $T=300$ K is narrower than the one obtained in an analogous MQW structure with ten periods only.²¹ This demonstrates the good structural uniformity of the present samples, in spite of the large number of QWs, and the reduced effect of interface roughness. For the first peak, attributed to the $\text{HH1-c}\Gamma 1$ transition, we mea-

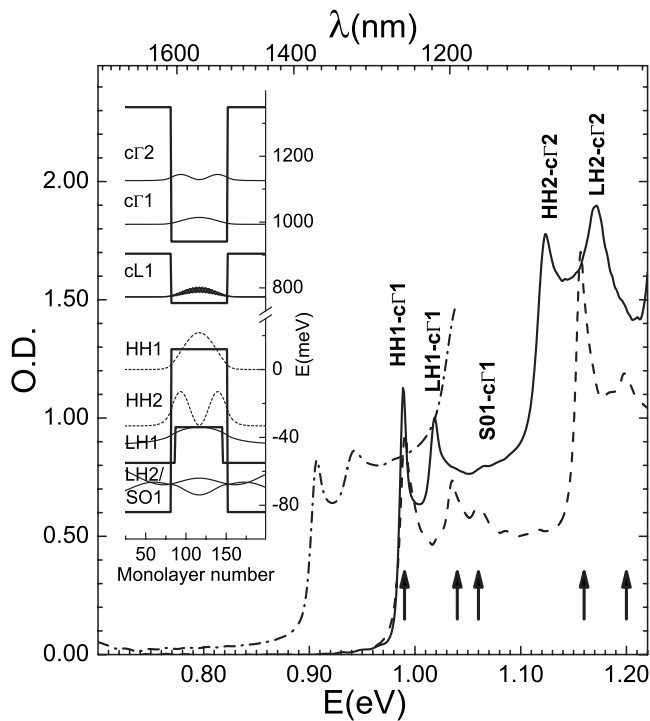


FIG. 1. Transmission spectra of the 7864-10 Ge/Si_{0.18}Ge_{0.82} 200 period MQW sample measured at 300 K (dashed-dotted line) and at 2 K (full line). The dashed line is the calculated low-temperature absorption spectrum. The arrows indicate the calculated transition energy between the QW states. In the inset the conduction and valence edge profiles and the square modulus of the wave functions of the electron- and hole-confined states are shown.

sure OD=1.1 at $T=2$ K. Considering that only the QWs absorb at this energy, a value for the absorption coefficient of about $1.3 \times 10^4 \text{ cm}^{-1}$ is obtained. This compares favorably with typical values for GaAs/AlGaAs QWs.²²

The high value of the OD and the sharp rise in the absorption edge, even at room temperature, are of interest also for applications of such structures in optical modulators. In fact, as shown in Ref. 21, in similar QWs an electric field on the order of 10^5 V m^{-1} along the growth direction induces a redshift of the absorption tail of about 30 meV. Given the room-temperature absorption spectrum in Fig. 1, we may thus expect a transmission modulation of few tenths of OD at 1400 nm upon the application of an electric field of 10^5 V m^{-1} . With MQWs of appropriate design, efficient light modulation at room temperature may even be feasible at 1550 nm.

In contrast to optical absorption, PL could be detected only at low temperature and high excitation intensity. This is probably due to the high density (10^6 – 10^7 cm^{-2}) of threading dislocations, typical of high Ge content SiGe alloys even when grown on graded VSs.²³ The PL spectrum of sample 7864-10 measured at $T=2$ K with an exciting power density $P_o \sim 3 \text{ kW cm}^{-2}$ is reported in Fig. 2. The spectrum is characterized by a line peaking at 0.978 eV, with a weak high-energy shoulder, and by a doublet composed of two narrower lines peaking at 0.740 and 0.768 eV, each with a low-energy shoulder. These two lines are superimposed onto the high-energy tail of a large structure stemming from recombination

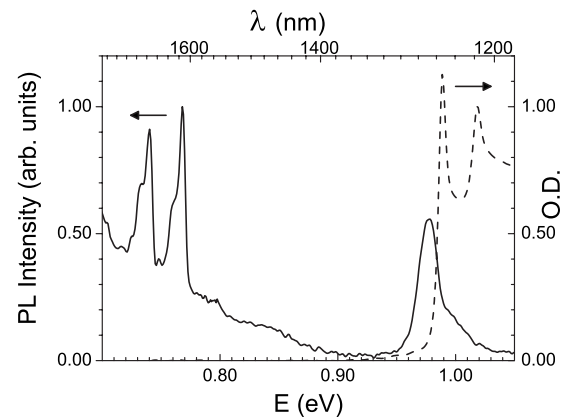


FIG. 2. Low-temperature PL spectrum of the 7864-10 Ge/Si_{0.18}Ge_{0.82} 200 QW sample measured at 2 K. PL was excited using the 1064 nm line of a Nd:YAG laser with an excitation power density of about 3 kW cm^{-2} . The 2 K transmission spectrum of the same sample is also reported (dashed line).

processes associated with extended defects, mainly dislocations.²⁴ The PL structure at 0.978 eV coincides with the low-energy tail of the transmission spectrum and thus can be attributed to the direct $c\Gamma_1$ -HH1 transition. The Stokes shift, which is the energy difference between the absorption peak and the PL peak, is about 11 meV and can be attributed mainly to QW width fluctuations.²⁵ With decreasing excitation intensity, the shoulder accompanying the 0.978 eV transition loses weight with respect to the main peak. For P below $\sim 0.7 \text{ kW cm}^{-2}$, it can no longer be detected. The energy separation of these two structures of about 20 meV rules out the attribution of the high-energy shoulder to the $c\Gamma_1$ -LH1 exciton recombination. The shoulder may be tentatively attributed to the modulation of the high-energy tail of the $c\Gamma_1$ -HH1 transitions due to self-absorption effects.

The low-energy PL doublet, at 0.740 and 0.768 eV for sample 7864-10 (Fig. 2), is present in the spectra of all samples. Its energy varies linearly with respect to the energy of the $c\Gamma_1$ -HH1 excitonic recombination, as shown in Fig. 3. This strongly suggests that these features are related to transitions between states confined in the MQWs. The spacing between the two lines does not depend on the energy and, thus, on the QW thickness. For each sample, also reported in Fig. 3 are the calculated transition energies between the lowest confined state at L in the CB, $cL1$, and the HH1 valence state plotted as a function of the calculated $c\Gamma_1$ -HH1 transition energy. In view of the good agreement in Fig. 3 between calculated and experimental values, we can attribute the high-energy line of the doublet to the $cL1$ -HH1 recombination. In the inset of Fig. 3, the experimental and the calculated energies of the $cL1$ -HH1 transition are reported as a function of the QW thickness. The good agreement between the experimental and calculated transition energies is therefore strong evidence for type-I band alignment of the L -type CB states and the Γ -type VB states in Ge QWs with Ge-rich SiGe barriers.

The intensity ratio of the two lines of the doublet at 0.740 and 0.768 eV remains constant over 6 orders of magnitude of the excitation power density. This strongly suggests that the

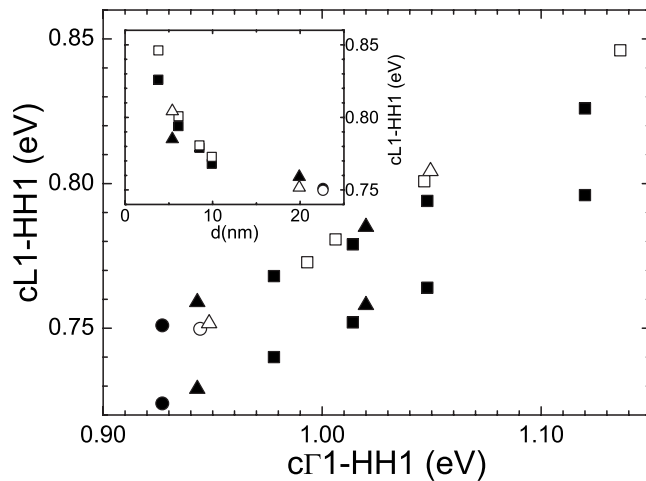


FIG. 3. Energy of the indirect $cL1$ -HH1 transitions and of its phonon replica as a function of the energy of the direct $c\Gamma1$ -HH1 transition. The data refer to samples cut from wafers 7873 (triangles), 7864 (squares), and 7909 (dots). The experimental data (filled symbols) are deduced from low-temperature PL spectra. The open symbols are the values calculated using the sample parameters reported in Table I. Excitonic effects have not been included in the calculations. In the inset the experimental and the calculated values of the energy of the indirect $cL1$ -HH1 transition are reported as a function of the Ge QW thickness.

lower-energy line is a phonon replica of the higher-energy line. Also the low-energy shoulders of both lines may be phonon replicas, as their energy shift from the main peak is much larger than the splitting expected from one monolayer

thickness change. The latter was evaluated to be less than 1 meV for the indirect $cL1$ -HH1 transition. These conclusions are supported by the fact that the energy spacings between the line at 0.768 eV and the other structures of the doublet in Fig. 2 are compatible with the frequency of Ge phonons at the L point of the Brillouin zone.¹⁰

The assignment of the 0.977 and 0.768 eV PL peaks in Fig. 2 to direct $c\Gamma1$ -HH1 and indirect $cL1$ -HH1 transitions, respectively, is supported by the observation that their intensity ratio decreases with their energy separation (not shown). The fact that they can be observed at all in the same PL spectrum follows from the close Γ and L CB minima in bulk Ge, lying at $E_{\Gamma}^{\text{gap}}=0.898$ eV and $E_L^{\text{gap}}=0.744$ eV at low temperature, respectively,¹⁰ and from the higher radiative recombination rate of the Γ - Γ transitions with respect to the Γ - L transitions. Indeed, both transitions have been observed simultaneously also in bulk Ge samples.²⁶

In conclusion, in this Rapid Communication we have presented transmission and PL experimental spectra of Ge MQWs between Ge-rich barriers grown by LEPECVD. A tight-binding model has been exploited to interpret the spectral features in terms of the electronic states of the analyzed samples. Our low-temperature PL spectra provide experimental confirmation of the predicted type-I band alignment in Ge/SiGe MQWs with Ge-rich barriers. Furthermore, the high quality of the grown samples and the corresponding sharp transmission spectra open other perspectives for applications of such heterostructures in near-infrared optical modulators.

The financial support of the Cariplo Foundation through the SIMBAD Project is gratefully acknowledged.

- ¹R. People and J. Bean, *Appl. Phys. Lett.* **48**, 538 (1986).
- ²D. C. Houghton, G. C. Aers, S. R. Eric Yang, E. Wang, and N. L. Rowell, *Phys. Rev. Lett.* **75**, 866 (1995).
- ³Y. Miyake, J. Y. Kim, Y. Shiraki, and S. Fukatsu, *Appl. Phys. Lett.* **68**, 2097 (1996).
- ⁴M. L. W. Thewalt, D. A. Harrison, C. F. Reinhart, J. A. Wolk, and H. Lafontaine, *Phys. Rev. Lett.* **79**, 269 (1997).
- ⁵J. C. Sturm, H. Manoharan, L. C. Lenchyshyn, M. L. W. Thewalt, N. L. Rowell, J. P. Noel, and D. C. Houghton, *Phys. Rev. Lett.* **66**, 1362 (1991).
- ⁶S. Fukatsu, H. Yoshida, N. Usami, A. Fujiwara, Y. Takahashi, Y. Siraki, and R. Ito, *Jpn. J. Appl. Phys., Part 2* **31**, L1319 (1992).
- ⁷N. L. Rowell, G. C. Aers, H. Lafontaine, and R. L. Williams, *Thin Solid Films* **321**, 158 (1998).
- ⁸F. Schäffler, *Semicond. Sci. Technol.* **12**, 1515 (1997).
- ⁹H. von Känel, M. Kummer, G. Isella, E. Müller, and T. Hackbarth, *Appl. Phys. Lett.* **80**, 2922 (2002).
- ¹⁰*Numerical Data and Functional Relationships in Science and Technology*, Landolt-Börnstein, New Series, Group III, Vol. 17, Pt. A, edited by O. Madelung (Springer-Verlag, Berlin, 1982).
- ¹¹Y.-H. Kuo, Y. K. Lee, Y. Ge, S. Ren, J. E. Roth, T. I. Kamins, D. A. B. Miller, and J. S. Harris, *Nature (London)* **437**, 1334 (2005).
- ¹²S. Tsujino, H. Sigg, G. Mussler, D. Chrastina, and H. von Känel, *Appl. Phys. Lett.* **89**, 262119 (2006).
- ¹³M. M. Rieger and P. Vogl, *Phys. Rev. B* **48**, 14276 (1993).
- ¹⁴M. Virgilio and G. Grosso, *J. Phys.: Condens. Matter* **18**, 1021 (2006).
- ¹⁵K. Driscoll and R. Paiella, *Appl. Phys. Lett.* **89**, 191110 (2006).
- ¹⁶W. H. Lau, V. Sih, N. P. Stern, R. C. Myers, D. A. Buell, A. C. Gossard, and D. D. Awschalom, *Appl. Phys. Lett.* **89**, 142104 (2006).
- ¹⁷H. Kosaka, H. Shigyou, Y. Mitsumori, Y. Rikitake, H. Imamura, T. Kutsuwa, K. Arai, and K. Edamatsu, *Phys. Rev. Lett.* **100**, 096602 (2008).
- ¹⁸M. Virgilio and G. Grosso, *Phys. Rev. B* **75**, 235428 (2007).
- ¹⁹J. M. Jancu, R. Scholz, F. Beltram, and F. Bassani, *Phys. Rev. B* **57**, 6493 (1998).
- ²⁰R. Dingle, W. Wiegmann, and C. H. Henry, *Phys. Rev. Lett.* **33**, 827 (1974).
- ²¹Y.-H. Kuo, Y. K. Lee, Y. Ge, S. Ren, J. E. Roth, T. I. Kamins, D. A. B. Miller, and J. S. Harris, *IEEE J. Sel. Top. Quantum Electron.* **12**, 1503 (2006).
- ²²W. T. Masselink, P. J. Pearah, J. Klem, C. K. Peng, H. Morkoc, G. D. Sanders, and Y. C. Chang, *Phys. Rev. B* **32**, 8027 (1985).
- ²³S. Marchionna, A. Virtuani, M. Acciarri, G. Isella, and H. von Känel, *Mater. Sci. Semicond. Process.* **9**, 802 (2006).
- ²⁴K. Tanaka, M. Suezawa, and I. Yonenaga, *J. Appl. Phys.* **80**, 6991 (1996).
- ²⁵A. Polimeni, A. Patane, M. Grassi Alessi, M. Capizzi, F. Martelli, A. Bosacchi, and S. Franchi, *Phys. Rev. B* **54**, 16389 (1996).
- ²⁶J. R. Haynes, *Phys. Rev.* **98**, 1866 (1955).